Zel'dovich Amplification in a Superconducting Circuit

Maria Chiara Braidotti[1,*] Andrea Vinante,[2,3] Giulio Gasbarri,[2] Daniele Faccio,[1] and Hendrik Ulbricht[2,†]

[1]*School of Physics and Astronomy, University of Glasgow, G12 8QQ Glasgow, United Kingdom*
[2]*Department of Physics and Astronomy, University of Southampton, SO17 1BJ Southampton, United Kingdom*
[3]*Istituto di Fotonica e Nanotecnologie–CNR and Fondazione Bruno Kessler, I-38123 Povo, Trento, Italy*

Zel'dovich proposed that electromagnetic (EM) waves with angular momentum reflected from a rotating metallic, lossy cylinder will be amplified. However, we are still lacking a direct experimental EM-wave verification of this fifty-year-old prediction due to the challenging conditions in which the phenomenon manifests itself: the mechanical rotation frequency of the cylinder must be comparable with the EM oscillation frequency. Here, we propose an experimental approach that solves this issue and is predicted to lead to a measurable Zel'dovich amplification with existing superconducting circuit technology. We design a superconducting circuit with low frequency EM modes that couple through free space to a magnetically levitated and spinning microsphere placed at the center of the circuit. We theoretically estimate the circuit EM mode gain and show that rotation of the microsphere can lead to experimentally observable amplification, thus paving the way for the first EM-field experimental demonstration of Zel'dovich amplification.

Zel'dovich predicted the amplification of electromagnetic (EM) waves scattering off a spinning metallic cylinder [1,2], showing that the rotational energy of a spinning body can be transferred to the EM modes if the body spins rapidly enough, i.e., when

$$\omega < q\Omega, \tag{1}$$

where Ω is the cylinder rotation frequency and ω and q are the frequency and the order of the angular momentum of the incident EM radiation.

The importance of this effect, aside from its own intrinsic interest, lies in the tight connection to other phenomena, from superradiant scattering, i.e., amplification of waves from a rotating black hole as predicted by Penrose [3] to Hawking radiation, i.e., evaporation of energy from a static black hole due to the interaction with quantum fluctuations [4]. Whereas laboratory analogs for these latter effects have been shown [5–9], we are still lacking experimental verification of Zel'dovich's idea, as originally proposed with EM waves. This appears to be simply due to a technological difficulty in satisfying the condition in Eq. (1), which nevertheless forces one to go back to carefully reexamine the underlying physical principles in order to propose a feasible experimental realization.

Beyond Zel'dovich's original proposal, Bekenstein suggested to confine the EM mode in a cavity surrounding the metallic cylinder [10] so as to resonantly increase the amplification effect. More recently, Gooding et al. [11] proposed to impinge on the rotating disk from the direction of the rotation axis, therefore harnessing the geometrical advantage of the dragging forces due to the penetration depth of the field inside the spinning body, as also suggested for acoustic experiments [12,13]. However, this proposal also remains challenging [11], requiring a macroscopic body to spin at tens of gigahertz.

In this Letter, we describe a method to perform the original Zel'dovich experiment aimed at observing amplification of EM waves from a conductive rotating body.

In more detail, we theoretically study the scattering from a rotating, levitated sphere of an EM mode that has angular momentum, i.e., in particular orbital angular momentum. We show analytically how the amount of gain measured in the reflected EM mode depends on the choice of the sphere material. We consider both a conductive nonmagnetic particle and a nonconductive ferromagnetic particle, showing that the predicted gain should be observable in a real experiment.

The proposed system consists of a levitated conductive microsphere stably spinning at frequency Ω and a rotating EM mode used to probe the Zel'dovich effect. Our proposed experimental setup is schematically shown in Fig. 1. The EM field is the EM mode of a superconducting circuit that is composed of four microcoils of equal inductance L. These microcoils are near-field coupled to the spinning, free space (i.e., not in physical contact with the circuit) microsphere. The microcoils are joined by transmission lines of equal length $\ell/4$ in a closed loop thus forming a closed circuit (see Fig. 1). The chosen geometry, and in particular the length of wire between each coil, is such that adjacent microcoils are phase shifted by $\pi/2$ allowing propagating and counterpropagating normal
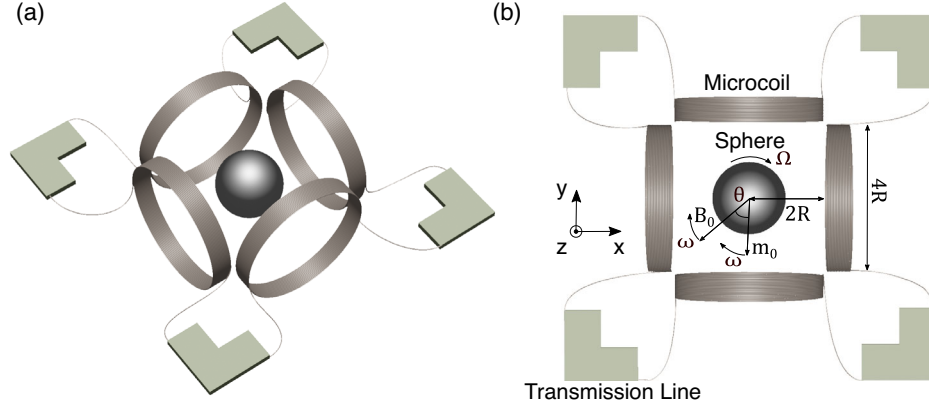
FIG. 1. (a) 3D Experimental setup. (b) Top view: the superconducting circuit is divided in four sections of length $\ell/4$, connected by four inductors with inductance L to form a closed ring configuration. The four coils have diameter equal to $4R$, where R is the radius of the central sphere, rotating at frequency Ω. The distance between each coil and the center of the sphere is $2R$. The arrows denote the magnetic field $\boldsymbol{B}_0$ generated by the four coils and the momentum $\boldsymbol{m}_0$ induced on the sphere. Both vectors rotate at frequency ω. θ is the angle between $\boldsymbol{B}_0$ and $\boldsymbol{m}_0$ and is related to the EM power dissipated in the sphere.

modes of EM frequency $\omega = ck_q$, where c is the speed of light in vacuum, $k_q = 2\pi q/\ell$, and nonzero orbital angular momentum $q = 1$ inside the circuit.

The whole system is placed in a cryogenic vacuum chamber at pressures of $\sim 10^{-5}$ mbar to enable low temperature measurements at $T \sim 4.2$ K (liquid helium temperature) or less, needed for superconducting technology and to obtain high electrical conductivities.

The initial driving to set the sphere in rotation is performed by switching the coil to an external circuit (not shown in Fig. 1). This driving magnetic field is generated by four waveform generators, each synchronized with a $\pi/2$ phase shift, thus following the procedure demonstrated in [14,15]. The driving field oscillates at a frequency ω_d and induces the microsphere to rotate at a frequency $\Omega \lesssim \omega_d$. Ω can also be tuned by changing the intensity of the driving field [14,15]. The maximum spinning frequency achievable with such a technique is only limited by the centrifugal forces overcoming the material stress limit and increases for decreasing sphere radius. For example, MHz rotation rates have been achieved by Schuck et al. with metallic spheres with a diameter of 0.5 mm [15].

Once the sphere reaches the desired rotation frequency the driving circuit and function generators are electronically switched off and probing is performed using the closed superconducting circuit shown in Fig. 1. In a vacuum of $\sim 10^{-5}$ mbar, we estimate that the levitated sphere will spin freely for more than one hour [15–17] (see Supplemental Material [18]), thus providing time to perform measurements with the superconducting circuit EM modes, under the assumption that these are significantly weaker than the driving EM field.

Theoretical analysis of the proposed system.—The probe EM field is generated by a sinusoidal current passing through the inductors. The current in the jth lumped inductor, corresponding to a propagating mode in the superconducting circuit, can be expressed as

$$I_j(t) = \bar{I}e^{i(k_q\xi_j - \omega t - \phi_0)}, \tag{2}$$

where $\xi_j = j\ell/4$ denotes the coordinate of the position of each coil along the line and $j = (0, 1, 2, 3)$. ϕ_0 is an initial random phase and $\bar{I}$ is the peak current flowing in the coils due to the propagating wave. The current flowing in the circuit can be measured by a SQUID, weakly coupled through a small inductance in series with the circuit (not shown in Fig. 1).

In the chosen configuration, the total probe magnetic field induced by the coils can be written by means of the Biot-Savart formula for a circular loop as [23]

$$\boldsymbol{B}_0 = 2\beta\bar{I}\boldsymbol{b}_0, \qquad \beta = \frac{N\mu_0}{8\sqrt{2}}\frac{1}{R}, \tag{3}$$

where $\boldsymbol{b}_0 = (1, i, 0)^T e^{i\omega t}$, R is the radius of the microsphere, N is the number of loops of each coil and the factor 2 accounts for the contribution of the two opposite-facing coils. We observe that $\boldsymbol{B}_0$ is complex. In Eq. (3), we chose an arrangement of four microcoils with radius $2R$ placed at a distance $2R$ from the center of the sphere [see Fig. 1(b)]. This geometrical configuration has been chosen to maximize the coupling between the sphere and the coils. These parameters are also compatible with current technology: superconducting niobium planar coils with $R \sim 100$ μm and high N, i.e., $N \sim 40$, can be fabricated using standard lithographic techniques and are typically used as input coils in conventional SQUIDs [24].

For simplicity the magnetic flux density $\boldsymbol{B}_0$ produced by the coils is assumed to be uniform over the microsphere volume, and the factor β in Eq. (3) is obtained by neglecting the thickness of each inductor. Thicker coils can also be

considered, replacing the parameter β by an effective β_{eff} averaged over different loop. However, planar coils, having a large turn density, are the best candidates for this experiment [25]. An example of a planar coil that can be fabricated with existing technology showing β_{eff} close to β is reported in the Supplemental Material [18]. We assume the spinning sphere axis is oriented along z, with the origin of the transverse (x, y) plane set in the center of the sphere [see Fig. 1(b)]. In the reference frame corotating with the microsphere, the magnetic flux density can be written as $\boldsymbol{B}_r = 2\beta\bar{\boldsymbol{l}}\boldsymbol{b}_r$ with $\boldsymbol{b}_r = (1, i, 0)^T e^{i\omega_r t}$ and where $\omega_r = \omega - \Omega$ is the frequency of the field in the corotating reference frame. From the definition of ω_r we can see that a negative corotating frequency will satisfy the Zel'dovich condition Eq. (1) for $q = 1$ that can be expressed as $\omega_r = \omega - \Omega < 0$: we will show that when $\omega_r < 0$, the effective dissipation becomes negative, implying a conversion of rotational mechanical energy into energy of the circuit electromagnetic mode.

The interaction between the magnetic probe field and the rotating sphere induces a magnetic dipole moment $\boldsymbol{m}_0$ on the sphere, which in the laboratory frame can be written as

$$\boldsymbol{m}_0 = \chi\boldsymbol{B}_0 = (\chi' + i\chi'')\boldsymbol{B}_0, \qquad (4)$$

where $\chi(\omega_r)$ is the complex response function of the sphere to the presence of the field in the corotating reference frame. The two vectors $\boldsymbol{m}_0$ and $\boldsymbol{B}_0$ rotate at the same EM frequency ω with an angular phase lag $\theta(\omega_r)$ determined by the imaginary part of the response function $\chi''(\omega_r)$ [see Fig. 1(b)], which gives rise to dissipation. If the sphere is conductive and nonmagnetic, χ depends on the electric conductivity $\sigma(\omega_r)$ whereas for a ferromagnetic ($\sigma = 0$) sphere, χ is proportional to the complex relative permeability $\mu_r(\omega_r)$ (see details in the Supplemental Material [18]).

The EM power dissipated by the sphere can be calculated as

$$W = \frac{1}{2}\Re\left\{-\boldsymbol{m}_0\frac{d\boldsymbol{B}_0^*}{dt}\right\} = 4\beta^2\omega\chi''(\omega_r)I_0^2, \qquad (5)$$

where the factor $1/2$ accounts for the average over one cycle, $\Re\{\cdot\}$ is the real part of the quantity in bracket, while $\boldsymbol{B}_0^*$ denotes the complex conjugate of the field [26]. The susceptibility $\chi(\omega_r)$ is the Fourier transform of the real-valued linear response function $\chi(t)$, which implies that $\chi''(-\omega_r) = -\chi''(\omega_r)$ [27]. A direct and key consequence of this is that when the Zel'dovich condition Eq. (1) is fulfilled, the power dissipated by the sphere becomes negative, i.e., power is radiated from the sphere into the EM circuit, leading to EM amplification.

The EM amplification can also be viewed as a result of the vector $\boldsymbol{m}_0$ preceding the vector $\boldsymbol{B}_0$, when $\omega_r < 0$ (rather than following it as usually happens when $\omega_r > 0$), as seen in the change of sign of rotation of the vector $\boldsymbol{m}_r$ in the

corotating frame. Under these conditions the torque applied by the EM field, given by $\boldsymbol{T} = \Re\{\boldsymbol{m}_0\} \times \Re\{\boldsymbol{B}_0\} = -|\boldsymbol{B}_0||\boldsymbol{m}_0|\sin(\theta)\hat{z}$, also becomes negative so that the EM field is extracting mechanical energy from the spinning sphere.

The total energy stored in the EM mode is $E = 1/2(L_0\ell + 4L)I_0^2$, where the first term is the energy stored in the transmission line and the second term is the energy stored in the four inductors. $L_0 = \sqrt{\varepsilon_r Z_0^2/c^2}$ is the transmission line inductance per unit length, where ε_r is the transmission line permittivity. The dissipation A, which is the key quantity we are interested in, can be finally expressed as the inverse of a quality factor Q:

$$A = Q^{-1} = \frac{W}{\omega E} = \frac{8\beta^2\chi''}{(L_0\ell + 4L)}. \qquad (6)$$

Under frequency inversion due to the Zel'dovich condition, χ'' and hence also A changes sign, so positive frequencies imply $A > 0$ while negative frequencies imply $A < 0$, i.e., gain.

We consider a rotating conductive microsphere with radius $R = 50\ \mu\text{m}$ and conductivity $\sigma \sim 5 \times 10^9\ \Omega^{-1}\,\text{m}^{-1}$, i.e., similar to that of common copper (residual resistance ratio ≈ 100) at $T = 4 - 10\ \text{K}$ [28]. These parameters lead to rotational frequencies in the megahertz range. This choice derives from a trade-off between conflicting requirements in the proposed experiment: a not too small sphere size to be compatible with existing fabrication and levitation technologies, and a high enough frequency ω to use transmission lines with realistic length. Figure 2 shows the predicted dissipation A induced by the microsphere obtained as a function of the EM frequency, ω, and rotation frequency Ω. Figure 2 clearly shows a transition from absorption to amplification when ω approaches the sphere rotation frequency Ω, thus showing evidence of a relatively strong Zel'dovich amplification that should be readily observable. Indeed, for $\omega > \Omega$, $A > 0$, i.e., the particle absorbs the magnetic radiation impinging on it as expected. On the other hand, for $\omega < \Omega$, A becomes negative, and hence the $\boldsymbol{B}$ field is amplified when scattered from the rotating sphere.

Fixing a feasible microsphere rotation frequency at $\Omega/2\pi = 2.5\ \text{MHz}$, we predict a maximum negative dissipation (i.e., gain) of $A_{\text{max}} \simeq -2 \times 10^{-3}$ [see Fig. 2(b) showing a line out from Fig. 2(a) along the white dashed line at $\Omega/2\pi = 2.5\ \text{MHz}$]. We note that the chosen frequency is below the fundamental limit to the maximum rotation frequency Ω_{max} that is determined by the sphere breaking apart. The breaking frequency scales with the inverse of radius and for $R = 50\ \mu\text{m}$ we estimate $\Omega_{\text{max}}/2\pi \approx 3.5\ \text{MHz}$, indicated in Fig. 2(a) by the dot-dashed black line. The red shaded area denotes the physically inaccessible region of frequencies due to the breaking of the microsphere [15]. The scaling of the
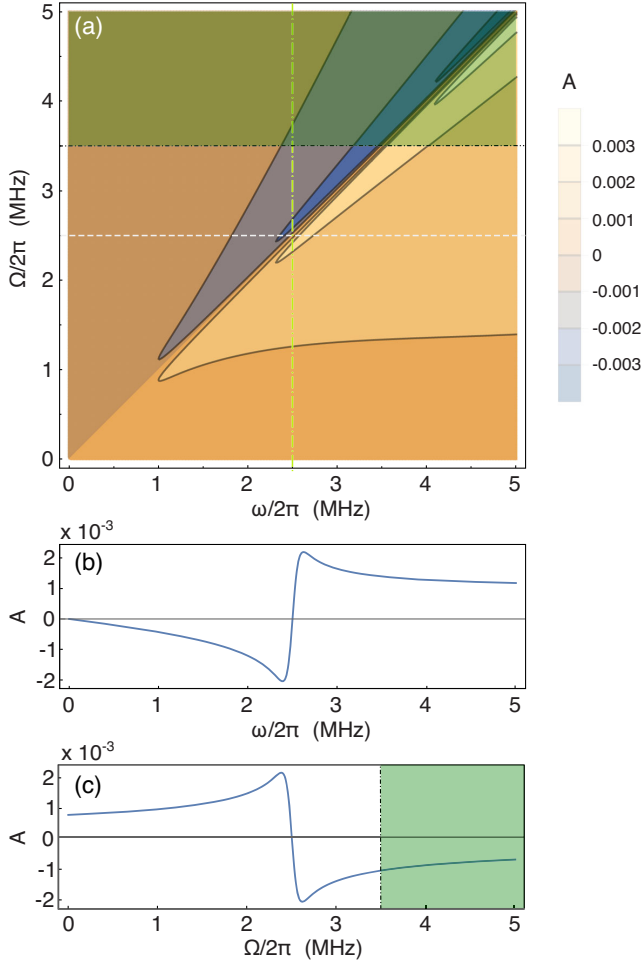
FIG. 2. (a) Rotational dissipation A as function of the magnetic field and sphere frequencies $\omega/2\pi$ and $\Omega/2\pi$. (b) A vs $\omega/2\pi$ for a fixed sphere rotation frequency $\Omega/2\pi = 2.5$ MHz of the particle [white dashed line in Fig. 2(a)]. (c) A vs $\Omega/2\pi$, fixing the field frequency $\omega/2\pi = 2.5$ MHz of the particle [green dot-dashed line in Fig. 2(a)]. In panels (a) and (c) the dot-dashed black line denotes the microsphere maximum rotations frequency $\Omega_{max}/2\pi = 3.5$ MHz and the green shaded area denotes the inaccessible region of frequencies. The parameters used are $\sigma = 5 \times 10^9 \ \Omega^{-1} \mathrm{m}^{-1}$, $\mu_r = 1$, $N = 40$, $Z_0 = 50 \ \Omega$, $R = 50 \ \mu\mathrm{m}$, $\ell = 74.8$ m, $\epsilon_r = 6.34$.

dissipation A as function of R can be found in the Supplemental Material [18].

Figure 2(c) shows the dissipation A trend for a fixed circuit frequency $\omega/2\pi = 2.5$ MHz as a function of the microsphere rotation frequency $\Omega/2\pi$.

Proposed experiment design details.—In an experiment, the EM mode frequency of 2.5 MHz can be obtained with a transmission line (see Fig. 1) formed by a compact coplanar waveguide of total length $\ell = |2\pi c/(\omega\sqrt{\varepsilon_r})| \sim 74.8$ m, where c is the speed of light and $\varepsilon_r = 6.38$ for a silicon substrate. Each section of the circuit will need to be $\ell/4 = 18.7$ m long. 2-m-long coplanar waveguides are routinely fabricated in superconducting kinetic inductance traveling amplifiers, on a typical chip area of 20×20 mm^2 [29,30]. These circuits are typically based on a double spiral geometry with constant pitch p, for which the area S is approximately proportional to the spiral length d by the relation $S = pd$. By scaling existing spiral design [30] a length of 18 m corresponds to a maximum radius of 3.8 cm. This is well within the current industrial standard for silicon wafers. This size is also compatible with standard commercial cryostats [31].

In order to evaluate the experimental observability of the amplification, we need to also compare A_{max} with all the other sources of dissipation A_0 in the electromagnetic modes, such as circuit losses. Meanderlike superconductive coplanar waveguides (i.e., the kinetic inductance traveling amplifiers proposed above) or microcoaxial niobium cables can be assumed to have $A_0^{\mathrm{wg}} \sim 10^{-5}$ [32–34]. Furthermore, microcoils in LC circuits show an intrinsic dissipation upper limit of $A_0^{\mathrm{coils}} \sim 10^{-4}$ [35]. These contributions are all more than one order of magnitude smaller than the gain predicted in Fig. 2 and are not expected to therefore contribute appreciably.

Other materials for the sphere may also be considered. For example, in the Supplemental Material [18] we show that a smaller amplification, of the order of 10^{-5}, can be achieved by magnetic particles of ferrite with moderate permeability $\mu_r \approx 900$ [36]. A similar analysis for the case of simultaneously conductive and magnetic materials (data not shown) leads to lower gain factors in comparison to the purely conductive case presented here. In the dielectric case, reported in the Supplemental Material [18], A is 5 orders of magnitude smaller due to limitations in the electric field amplitude that can be generated by capacitors (which now substitute the magnetic field and inductors, respectively).

We further observe that the particle does not need to be fully metallic. It can be a composite with a ferromagnetic core which allows an easier levitation [37] and a highly conductive coating such that the coating thickness is comparable to the penetration depth of the EM field (see Ref. [18]).

Conclusions.—We propose a superconducting circuit combined with a free space, rotating sphere that is coupled to the circuit: this provides efficient EM-sphere coupling at low EM frequencies which in turn allow the access of experimentally feasible rotational frequencies for the sphere, as required by the Zel'dovich condition.

Our calculations show that the proposed setup exhibits measurable amplification of EM waves from mechanical rotation of both metallic and magnetic particles. It is worth noting that if GHz rotation frequencies could be reached with a similar scheme, then the circuit can be cooled to millikelvin temperatures where the thermal population is negligible, i.e., $k_b T < \hbar\omega$, a condition which has enabled superconducting quantum electrodynamics (QED) [38] and the study of fundamental physical effects such as

dynamical Casimir emission [39,40]. Gigahertz rotation frequencies have been obtained with optical trapping of submicron sized spheres [41,42]. This would require arranging four nanocoils at a distance of ~100 nm from the particle, which is incompatible with a realistic trapping laser waist. Moreover, the combination of a high power laser beam with a millikelvin environment would require careful control of heat dissipation aspects. However, if these technological issues can be solved, spontaneous Zel'dovich emission could then also be observed, i.e., rotational generation of photons out of the quantum vacuum [1] in a superconducting QED experiment. In addition, the system proposed here relies on a new generation of superconducting circuits coupled to rapidly moving elements, thus allowing the study of further fundamental physics problems such as the detection of rotational quantum friction [43–45] and quantum vacuum friction [46].

---

[*] mariachiara.braidotti@glasgow.ac.uk

[†] h.ulbricht@soton.ac.uk

[1] Y. B. Zel'dovich, Generation of waves by a rotating body, Pis'ma Zh. Eksp. Teor. Fiz. **14**, 270 (1971) [JETP Lett. **14**, 180 (1971)].

[2] Y. B. Zel'dovich, Amplification of cylindrical electromagnetic waves reflected from a rotating body, Zh. Eksp. Teor. Fiz. **62**, 2076 (1972) [Sov. Phys. JETP **35**, 1085 (1972)].

[3] R. Penrose, Gravitational collapse: The role of general relativity, Gen. Relativ. Gravit. **34**, 1141 (2002), reprinted from Rivista del Nuovo Cimento, Numero Speziale **I**, 25 (1969).

[4] S. Hawking, Black hole explosions?, Nature (London) **248**, 30 (1974).

[5] G. Rousseaux, C. Mathis, P. Massa, T. G. Philbin, and U. Leonhardt, Observation of negative-frequency waves in a water tank: A classical analogue to the Hawking effect?, New J. Phys. **10**, 053015 (2008).

[6] T. Torres, S. Patrick, A. Coutant, M. Richartz, E. W. Tedford, and S. Weinfurtner, Rotational superradiant scattering in a vortex flow, Nat. Phys. **13**, 833 (2017).

[7] Silke Weinfurtner, Edmund W. Tedford, Matthew C. J. Penrice, William G. Unruh, and Gregory A. Lawrence, Measurement of Stimulated Hawking Emission in an Analogue System, Phys. Rev. Lett. **106**, 021302 (2011).

[8] J. Steinhauer, Observation of quantum Hawking radiation and its entanglement in an analogue black hole, Nat. Phys. **12**, 959 (2016).

[9] J. R. M. de Nova, K. Golubkov, V. I. Kolobov, and J. Steinhauer, Observation of thermal Hawking radiation and its temperature in an analogue black hole, Nature (London) **569**, 688 (2019).

[10] J. D. Bekenstein and M. Schiffer, The many faces of superradiance, Phys. Rev. D **58**, 064014 (1998).

[11] C. Gooding, S. Weinfurtner, and W. G. Unruh, Reinventing the Zel'dovich wheel, Phys. Rev. A **101**, 063819 (2020).

[12] D. Faccio and E. M. Wright, Superradiant Amplification of Acoustic Beams via Medium Rotation, Phys. Rev. Lett. **123**, 044301 (2019).

[13] C. Gooding, S. Weinfurtner, and W. G. Unruh, Superradiant scattering of orbital angular momentum beams, arXiv:1809.08235.

[14] T. Reichert, T. Nussbaumer, and J. W. Kolar, Complete analytical solution of electromagnetic field problem of high-speed spinning ball, J. Appl. Phys. **112**, 104901 (2012).

[15] M. Schuck, D. Steinert, T. Nussbaumer, and J. W. Kolar, Ultrafast rotation of magnetically levitated macroscopic steel spheres, Sci. Adv. **4**, e1701519 (2018).

[16] D. H. Gabis, S. K. Loyalka, and T. S. Storvick, Measurements of the tangential momentum accommodation coefficient in the transition flow regime with a spinning rotor gauge, J. Vac. Sci. Technol. A **14**, 2592 (1996).

[17] P. S. Epstein, On resistance experienced by spheres in their motion through gases, Phys. Rev. **23**, 710 (1924).

[18] See Supplemental Material at http://link.aps.org/supplemental/10.1103/PhysRevLett.125.140801 for additional information on the penetration depth and the calculations of the dissipation A with a ferromagnetic microsphere and a dielectric one, which includes Refs. [19–22].

[19] R. P. Feynman, R. B. Leighton, and M. Sands, *The Feynman Lectures on Physics* (Addison Wesley, Redwood City, 2005).

[20] Magnetics, https://www.mag-inc.com/.

[21] J. P. Cosier and R. F. Pearson, Low-temperature permeability measurements on ferrites, Br. J. Appl. Phys. **18**, 615 (1967).

[22] N. S. Midi, K. Sasaki, R. Ohyama, and N. Shinyashiki, Broadband complex dielectric constants of water and sodium chloride aqueous solutions with different DC conductivities, IEEJ Trans. Electr. Electron. Eng. **9**, 8 (2014).

[23] D. J. Griffiths, *Introduction to Electrodynamics*, 3rd ed. (Prentice Hall, Upper Saddle River, 1999).

[24] J. Clarke and A. I. Braginski, *The SQUID Handbook* (Wiley-VCH Verlag GmbH and Co., Weinheim, 2004).

[25] M. Peruzzo, A. Trioni, F. Hassani, M. Zemlicka, and J. M. Fink, Surpassing the resistance quantum with a geometric superinductor, arXiv:2007.01644v1.

[26] L. D. Landau and E. M. Lifshitz, *Electrodynamics of Continuous Media*, 2nd ed. (Pergamon Press, New York, 1984).

[27] L. D. Landau and E. M. Lifshitz, *Statistical Physics*, 3rd ed. (Pergamon Press, New York, 1980).

[28] https://www.copper.org/resources/properties/cryogenic/.

[29] L. Ranzani, M. Bal, K. C. Fong, G. Ribeill, X. Wu, J. Long, H.-S. Ku, R. P. Erickson, D. Pappas, and T. A. Ohki, Kinetic inductance traveling-wave amplifiers for multiplexed qubit readout, Appl. Phys. Lett. **113**, 242602 (2018).

[30] B. Ho Eom, P. K. Day, H. G. LeDuc, and J. Zmuidzinas, A wideband, low-noise superconducting amplifier with high dynamic range, Nat. Phys. **8**, 623 (2012).

[31] https://schoonoverinc.com/vacuum-maintenance/laboratory-cryo-cooler/custom-chamber-cryocooler/.

[32] Aaron D. O'Connell, M. Ansmann, Radoslaw C. Bialczak, Max Hofheinz, Nadav Katz, Erik Lucero, C. McKenney, Matthew Neeley, Haohua Wang, Eva M. Weig *et al.*, Microwave dielectric loss at single photon energies and millikelvin temperatures, Appl. Phys. Lett. **92**, 112903 (2008).

[33] J. Zmuidzinas, Superconducting microresonators: Physics and Applications, Annu. Rev. Condens. Matter Phys. **3**, 169 (2012).

[34] P. Kurpiers, T. Walter, P. Magnard, Y. Salathe, and A. Wallraff, Characterizing the attenuation of coaxial and rectangular microwave-frequency waveguides at cryogenic temperatures, Eur. Phys. J. Quantum Technol. **4**, 8 (2017).

[35] L. Gottardi, J. van der Kuur, M. Bruijn, A. van der Linden, M. Kiviranta, H. Akamatsu, R. den Hartog, and K. Ravensberg, Intrinsic losses and noise of high-Q lithographic MHz LC resonators for frequency division multiplexing, J. Low Temp. Phys. **194**, 370 (2019).

[36] https://www.pptechnology.com/.

[37] A. Vinante, P. Falferi, G. Gasbarri, A. Setter, C. Timberlake, and H. Ulbricht, Ultralow mechanical damping with Meissner-levitated ferromagnetic microparticles, Phys. Rev. Applied **13**, 064027 (2020).

[38] X. Gu, A. Frisk Kockum, A. Miranowicz, Y. Liu, and F. Nori, Microwave photonics with superconducting quantum circuits, Phys. Rep. **718**, 1 (2017).

[39] C. M. Wilsonand G. Johansson, A. Pourkabirian, M. Simoen, J. R. Johansson, T. Duty, F. Nori, and P. Delsing, Observation of the dynamical Casimir effect in a superconducting circuit, Nature (London) **479**, 376 (2011).

[40] Pasi Lähteenmäki, G. S. Paraoanu, Juha Hassel, and Pertti J. Hakonen, Dynamical Casimir effect in a Josephson metamaterial, Proc. Natl. Acad. Sci. U.S.A. **110**, 4234 (2013).

[41] René Reimann, Michael Doderer, Erik Hebestreit, Rozenn Diehl, Martin Frimmer, Dominik Windey, Felix Tebbenjohanns, and Lukas Novotny, GHz Rotation of an Optically Trapped Nanoparticle in Vacuum, Phys. Rev. Lett. **121**, 033602 (2018).

[42] Jonghoon Ahn, Zhujing Xu, Jaehoon Bang, Yu-Hao Deng, Thai M. Hoang, Qinkai Han, Ren-Min Ma, and Tongcang Li, Optically Levitated Nanodumbbell Torsion Balance and GHz Nanomechanical Rotor, Phys. Rev. Lett. **121**, 033603 (2018).

[43] R. Zhao, A. Manjavacas, F. J. Garca de Abajo, and J. B. Pendry, Rotational Quantum Friction, Phys. Rev. Lett. **109**, 123604 (2012).

[44] A. Manjavacas and F. J. Garca de Abajo, Thermal and vacuum friction acting on rotating particles, Phys. Rev. A **82**, 063827 (2010).

[45] M. F. Maghrebi, R. L. Jaffe, and M. Kardar, Spontaneous Emission by Rotating Objects: A Scattering Approach, Phys. Rev. Lett. **108**, 230403 (2012).

[46] P. C. W. Davies, Quantum vacuum friction, J. Opt. B **7**, S40 (2005).